Powder Metallurgy Progress, Vol.16 (2016), No.2, p.86-98
http://dx.doi.org/10.1515/pmp-2016-0007

REACTION OF UNALLOYED AND Cr-Mo ALLOYED STEELS WITH NITROGEN FROM THE SINTERING ATMOSPHERE

M. Dlapka, Ch. Gierl-Mayer, R. O. Calderon, H. Danninger, S. Bengtsson, E. Dudrova

Abstract

Nitrogen is usually regarded as an inert sintering atmosphere for PM steels; however, this cannot be taken for granted in particular for steels alloyed with nitride forming elements. Among those elements, chromium has become more and more important as an alloying element in sintered low alloy structural steels in the last decade due to the moderate alloying cost and the excellent mechanical properties obtainable, in particular when sinter hardening is applied. The high affinity of Cr to oxygen and the possible ways to overcome related problems have been the subject of numerous studies, while the fact that chromium is also a fairly strong nitride forming element has largely been neglected at least for low alloy steel grades, although frequently used materials like steels from Cr and Cr-Mo prealloyed powders are commonly sintered in atmospheres consisting mainly of nitrogen.

In the present study, nitrogen pickup during sintering at different temperatures and for varying times has been studied for Cr-Mo prealloyed steel grades as well as for unalloyed carbon steel. Also the effect of the cooling rate and its influence on the properties, of the microstructure and the composition have been investigated. It showed that the main nitrogen uptake occurs not during isothermal sintering but rather during cooling. It could be demonstrated that a critical temperature range exists within which the investigated CrM-based steel is particularly sensitive to nitrogen pickup.

Keywords: powder metallurgy, sintering conditions, microstructure

INTRODUCTION

In the last years, the classical alloying elements for sintered steels, i.e. Ni, Cu and Mo, have been more and more replaced by cheaper alternatives such as Cr and Mn [1, 2]. These latter elements provide good hardenability at low cost, which makes them attractive alloying constituents for sinter hardening steel grades. Chromium (as well as manganese) is however sensitive to oxidation, and therefore sintering of steels containing Cr is a difficult task. The problem is that Cr forms stable oxides which weaken the sintering contacts if they are not reduced properly. Reducing these oxides is only possible at high sintering temperatures, with the presence of carbon as the main reducing agent even if sintering in H_2 containing atmospheres. This has been the task of numerous studies (e.g. [3, 4, 5]).

Magdalena Dlapka*, Christian Gierl-Mayer, Raquel de Oro Calderon, Herbert Danninger: Technische Universität Wien, Getreidemarkt 9//164 CT, A-1060 Vienna, Austria, (*now: MIBA Sinter Austria GmbH, A-4655 Vorchdorf, Austria)
Sven Bengtsson, Höganäs AB, Bruksgatan 35, S-263 83 Höganäs, Sweden
Eva Dudrova, Institute of Materials Research SAS, Watsonova 47, SK-040 01 Košice, Slovakia

Beside this, Cr has a strong tendency to form nitrides (e.g. [6, 7], which is one of the reasons why it is a main alloy element in nitriding grade steels, the other being the very positive effect on N solubility in Fe [8]. The nitrides appearing in the phase diagram Cr-N are Cr_2N (hcp) and CrN (fcc) [8]. These are also the stable nitrides formed when Fe and Fe+C are added to the system [9]. There are no separate carbonitride phases in Cr alloy steels described in [10], although Ettmayer mentioned orthorhombic carbonitrides for Cr-C-N [11]. However, Cr_2N has increasing solubility both for C and Fe at higher temperatures, i.e. the phase can then be described as $(Cr,Fe)_2(N,C)$, similar to the $Cr_2(C,N)$ given for the ternary system Cr-C-N [12].

Nitrogen is frequently used as a sintering atmosphere, either plain N_2 or combined with H_2, as e.g. forming gas N_2-10%H_2, which means that Cr is held at high temperatures for a long time in a 'non-inert atmosphere'. Already in 1971, Šalak pointed out that nitrogen containing atmospheres cannot be regarded as being "inert" even for sintering of plain iron parts [13], which has been experimentally corroborated e.g. in [14]. Furthermore, esp. for soft magnetic PM parts, e.g. Fe or Fe-P, using plain H_2 is recommended to avoid formation of fine nitride phases after cooling which increase the coercive force [15-17]. Anyway, nitrogen is still used like an inert atmosphere for most ferrous PM materials [18, 19]. There are only a few investigations checking this assumption, and these are mostly focusing on high alloy steels [20, 21]. Of course, the nitriding effect of the very stable triple-bonded molecular N_2 cannot be compared with the nascent N formed through dissociation of NH_3 in gas nitriding or through plasma assisted dissociation of N_2 in plasma nitriding [22]. On the other hand, sintered steels with standard density (7.3 $g.cm^{-3}$ maximum) exhibit almost exclusively open and interconnected porosity [23] and thus a much larger specific surface – and resulting reactivity – than wrought steels. Furthermore, the much higher temperatures during sintering compared with nitriding should be considered - >1100°C compared to about 500°C – which on one hand promote thermal dissociation of N_2, on the other hand also effusion of dissolved N from the metal matrix. The most pronounced effect is however the dramatlc change of the N solubility caused by the different Fe modifications [8]: the austenite present at sintering temperature has a much higher solubility for nitrogen than the ferrite present during nitriding.

In the present work, nitrogen pickup during sintering and the formation of nitrides in plain carbon steels as well as in Cr-Mo prealloyed steel compacts were investigated as a function of the sintering conditions (temperature, time, cooling rate), and the position of the nitrogen in the sintered material was identified. Furthermore it was checked if there is a critical temperature range in which nitrides are most likely to form.

EXPERIMENTAL PROCEDURE

The base powder for the investigations was prealloyed steel powder Fe-3%Cr-0.5%Mo (Astaloy CrM, Höganäs AB) admixed with natural graphite (Kropfmühl UF4, purified grade). Different amounts of carbon were added, namely in a first run a higher content of 0.7% and then 0.08 and 0.3%C (all concentrations given in mass%). The 0.08%C was added to obtain a well sintered material with hardly any oxygen (carbon being required as reducing agent, see [5]) and as low content of carbon as possible after sintering. The higher contents were chosen to check if there are any interactions between carbon and nitrogen in the material. Plain iron powder ASC 100.29 (Höganäs AB) was used as reference. After blending in a tumbling mixer, pressing was done at 600 MPa using die wall lubrication, to avoid any introduction of carbon through admixed lubricant. Sintering was carried out in a SiC rod heated pusher furnace with superalloy retort at 1120 or 1250 °C isothermal. Further specimens were sintered in a Netzsch DIL 402 C pushrod dilatometer

with a heating rate of 10 K/min followed by a holding time of 1 h and varying cooling rates (50 – 0.5 $K.min^{-1}$). In both sintering aggregates the sintering atmosphere was pure nitrogen or, as a truly inert reference, pure argon (99.999 % purity each).

Thermogravimetry was used to identify the temperature ranges within which the nitrogen pickup predominantly occurs. Therefore small pieces were heated to 1120 °C and cooled with different rates in a simultaneous thermal analyzer (DTA/TG) Netzsch STA 449. Also here, N_2 and Ar were used as atmospheres.

The oxygen and nitrogen contents, respectively, were measured through hot fusion analysis using a LECO TC 400 analyzer. For this, the samples were cut into small pieces of 0,2 to 1 g, done manually with a HSS saw blade in dry cut, to make sure that the preparation of the samples did not have any influence on the result (e.g. by oxidation, corrosion, carbon contamination etc.). Carbon analysis was done on a LECO CS-230 combustion analyzer.

The microstructure was characterized by metallographic methods, and the fracture surfaces were studied by SEM. The sectioned samples were ground and polished. The etching was accomplished with a Nital-Picral (4 g Picric acid in 100 ml methanol, 2 ml HNO_3 added) etching agent. The fracture surface was investigated on tested impact bars that had been broken at room temperature. The scanning electron microscope used for this was an SEM Thermal FEG Jeol JSM 7000F with an INCA x-sight 10 mm^2 Silicon detector EDS7557 at the Institute of Materials Research in Košice.

Furthermore, WDX analyses were done using a FEI XL30 ESEM with an Oxford Microspec WDX-600 Spectrometer.

Sintering studies

The fact that sintering in nitrogen has an effect on the chromium containing material Astaloy CrM was proven by dilatometric sintering runs performed in two different atmospheres, namely in pure nitrogen and pure argon. It is clearly evident that this chromium containing material picks up nitrogen if it is present in the sintering atmosphere (Table 1). In contrast to the pronounced differences of the nitrogen content (by a factor of about 250), the oxygen content is virtually identical, proving that carbothermal reduction of the oxides is not affected by the atmosphere, which agrees with previous experiments (see e.g. [5, 24]).

Tab.1. Nitrogen and oxygen content of Astaloy CrM-0.7%C sintered in the dilatometer in different atmospheres with a heating rate of 10 $K.min^{-1}$, 1 h isothermal at 1120°C and a cooling rate of 10 $K.min^{-1}$.

Sintering atmosphere	Nitrogen content [%]	Oxygen content [%]
Nitrogen	0.126 ± 0.004	0.0181 ± 0.0002
Argon	0.0005 ± 0.0004	0.017 ± 0.002

Due to this fact it was of interest which sintering parameters have the main influence on the nitrogen pickup. Therefore in a test series done in the pusher furnace the sintering temperature was varied (1120°C and 1250°C) as well as the isothermal sintering time (1 h, 4 h and 8 h) and, in dilatometric runs, the cooling rate (50 $K.min^{-1}$, 5 $K.min^{-1}$ and 0.5 $K.min^{-1}$, in the dilatometer). As stated above, Astaloy CrM was mixed with 0.08%C and with 0.3%C. The lower amount of carbon should result in almost carbon-free Astaloy CrM after sintering, due to the loss of carbon by carbothermal reduction, and the higher one should show if carbon present influences the nitrogen pickup significantly. Compacts from

plain iron ASC 100.29 (without carbon) were used as reference. The results of the test series sintered in the pusher furnace are shown in Table 2 and, to graphically illustrate the nitrogen pickup, in Fig.1.

Tab.2. Influence of the different sintering parameters (temperature and time) on the nitrogen content for plain iron (ASC) without carbon, Astaloy CrM-0.08%C and Astaloy CrM- 0.3%C sintered in the pusher furnace in pure N_2 with approx. 20-30 K.min^{-1} cooling rate (linearized).

	Nitrogen content [%]		
1120°C	1 h	4 h	8 h
ASC	0.027	0.026	0.027
CrM-0.08%C	0.061	0.065	0.062
CrM-0.3%C	0.058	0.062	0.061
1250°C	1 h	4 h	8 h
ASC	0.025	0,025	0,025
CrM-0.08%C	0.052	0,050	0,054
CrM-0.3%C	0.058	0,049	0,051

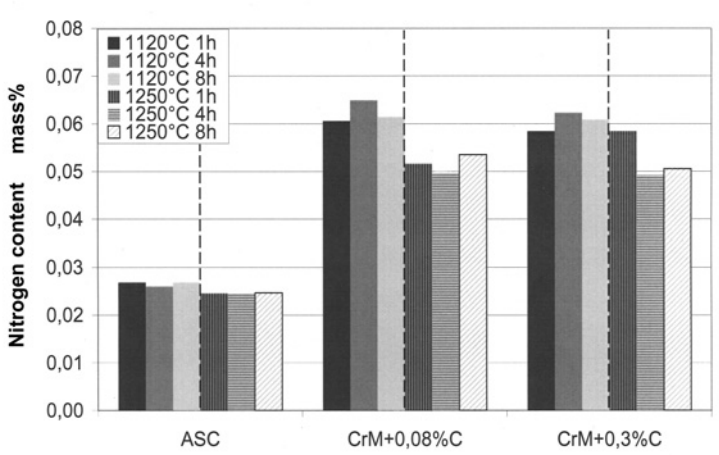

Fig.1. Influence of the different sintering parameters (temp., and time) on the nitrogen content for ASC, Astaloy CrM-0.08%C and Astaloy CrM-0.3%C sintered in high purity N_2 with cooling rate of 20-30 K.min^{-1} (linearized).

As clearly visible from Table 2 and Fig.1, the Cr-Mo containing Astaloy CrM-x%C picks up a significantly higher amount of nitrogen compared to the ASC based material which does not contain any nitride forming elements. Furthermore it is evident that the sintering time is more or less irrelevant. Sintering at 1120 °C resulted in slightly higher nitrogen contents compared to 1250 °C. The reason is the equilibrium which at higher temperatures favours the gaseous variant, i.e. nitrogen effusion [8]. The carbon content seems to be of minor relevance, at least at the cooling rate applied here.

In any case, comparison of Table 1 and Table 2, the results from the dilatometer (slow cooling) vs. the pusher furnace (fast cooling) indicates that the cooling rate plays a

major role. Therefore, the effect of the cooling rate after sintering was investigated by sintering in the dilatometer (Table 2). Thus it was possible to obtain constant and even very slow cooling rates under well defined conditions.

Tab.3. Nitrogen and carbon content of ASC and Astaloy CrM-x%C sintered 1 h at 1120°C in the dilatometer in flowing high purity N_2, cooled at rates of 50, 5 and 0.5 K.min^{-1}, respectively.

a) Nitrogen content

Material composition	50 K.min^{-1}	5 K.min^{-1}	0.5 K.min^{-1}
ASC	0.026 ± 0.0002	0.025 ± 0.001	0.016 ± 0.0001
CrM-0.08%C	0.064 ± 0.001	0.104 ± 0.001	0.342 ± 0.001
CrM-0.3%C	0.063 ± 0.0001	0.093 ± 0.0003	0.204 ± 0.005

b) Carbon content

Material composition	50 K.min^{-1}	5 K.min^{-1}	0.5 K.min^{-1}
CrM-0.08%C	0.032 ± 0.003	0.042 ± 0.004	0.020 ± 0.002
CrM-0.3%C	0.24 ± 0.01	0.214 ± 0.003	0.23 ± 0.02

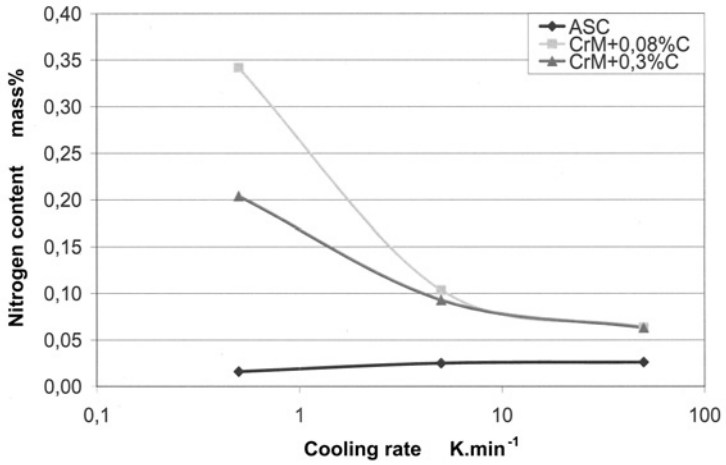

Fig.2. Nitrogen content as a function of the cooling rate. Dilatometer, 1120°C, N_2.

It is evident that the amount of nitrogen in the specimen strongly depends on the cooling rate from sintering temperature. Slower cooling results in much higher nitrogen levels in the material. With slower cooling there is also an increasingly pronounced effect of the carbon content: at slow cooling the low-carbon material (which after sintering in fact contains hardly any carbon at all, as evident from Table 3a) takes more nitrogen. The reason is the lower diffusion coefficient of nitrogen in iron for increasing carbon content due to the constraining of the nitrogen diffusion by the presence of carbon in the lattice [25].

The pronounced effect of the cooling rate strongly indicates that there is a critical temperature range in which nitrogen pickup occurs. The longer the material is held in this critical temperature range, the higher is the resulting nitrogen value. This can be assumed to be the reason why the materials cooled more slowly – which means that they remain in this critical temperature range for longer time - show the highest nitrogen values.

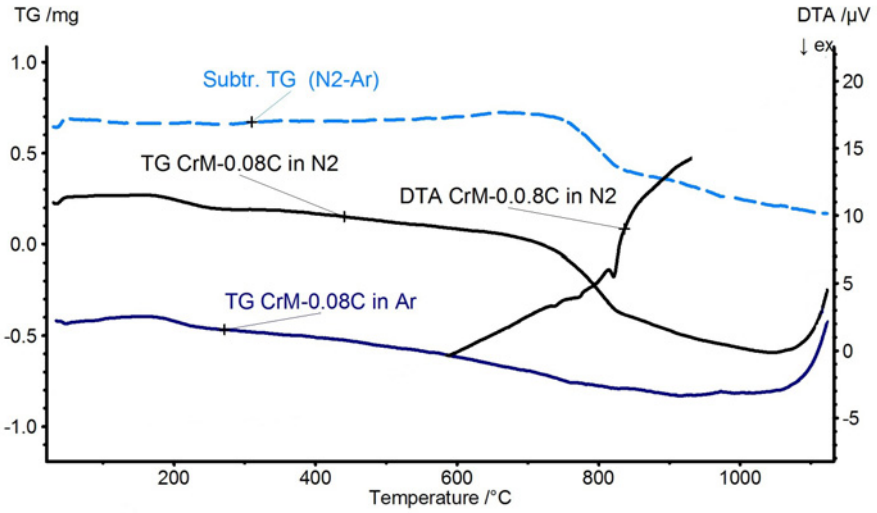

Fig.3. Critical temperature range for nitrogen pickup of Astaloy CrM-0.08%C during cooling at 0.5 K/min in STA after heating with 10 K.min^{-1} to 1250 °C and a holding time of 1 min at sintering temperature in N_2 or Ar.

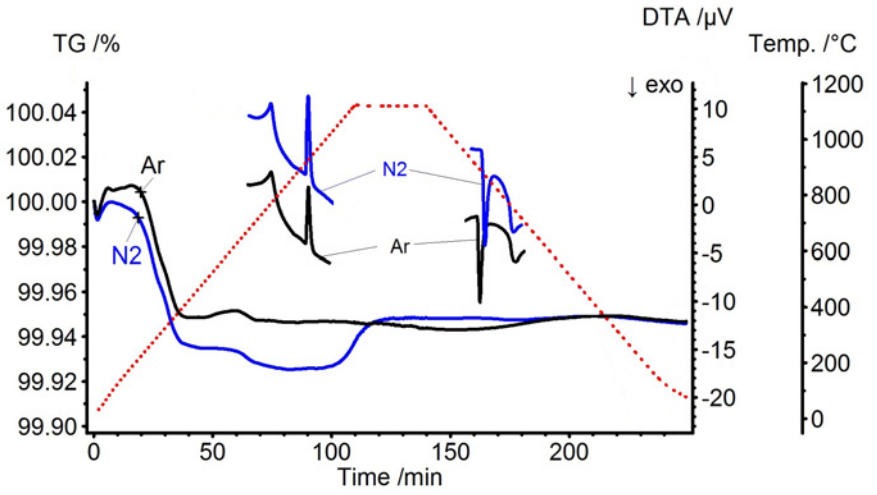

a) Thermogravimetry (inserts: DTA signal) of ASC 100.29

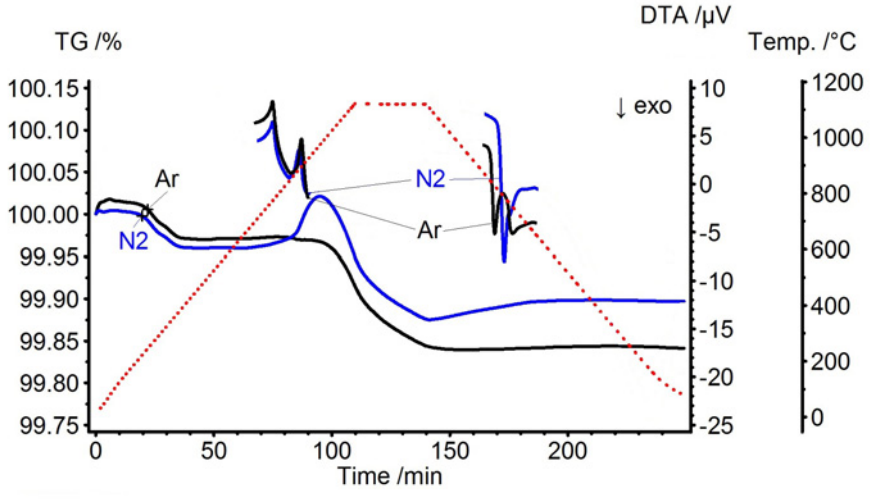

b) Thermogravimetry (inserts: DTA signal) Astaloy CrM-0.08%C

Fig.4a,b. TG and DTA-graphs (transformation area during cooling) of Astaloy CrM-0.08.%C and ASC100.20 in Ar and N_2, respectively. Heating/cooling rate $\pm$10 K min, 1120°C 30 min.

To identify this critical temperature range, a thermogravimetric analysis was performed in parallel in nitrogen and argon at 0.5 $K.min^{-1}$ cooling rate (Fig.3). There occurs a mass gain starting at 1120°C but with a pronounced jump at about 800°C which means that it is connected to the $\gamma \rightarrow \alpha$ transformation as indicated by the inserted section of the DTA graph, N uptake being apparently more pronounced below the transformation temperature. This is a rather surprising feature since with regard to the very low solubility of N in ferrite compared to austenite, rather N pickup in the lower austenite range would be expected. A practical problem with these analyses was that keeping the specimens for long times at high temperatures, which was the case if very slow cooling was done, resulted not only in pickup of nitrogen but also of oxygen, which also resulted in mass gain. Therefore it is difficult to distinguish between these two effects. It seems however that this oxidation effect occurs in both atmospheres, and since the subtracted curve (N_2-Ar) is flat in this area the nitriding effect can be verified.

The experiments shown in Fig. 4, done for both Fe and Fe-Cr-Mo matrices and at more standard heating and cooling rates, show that the mass change effect is much more pronounced when chromium is present as alloying element, and although the effect is less pronounced if cooling is performed much faster, the DTA shows a shift of the transformation in both cases, indicating presence of a strongly austenite stabilizing element (N). Interestingly, in the graph for Astaloy CrM a quite pronounced mass gain is observed during heating, and in this case it clearly starts from the onset of the $\alpha \rightarrow \gamma$ transformation (the second peak in the DTA heating graph; the first one indicates the Curie temperature). This is followed by an equally pronounced mass loss, indicating nitrogen effusion at higher temperatures (but of course also pronounced reduction, as indicated by the similar, though somewhat less pronounced, mass loss in Ar). This corroborates that nitrogen uptake of the Cr prealloy steels occurs actually in a relatively narrow temperature interval, both in heating and in cooling.

From the practical viewpoint it might be assumed that this N uptake during cooling is not too much of a problem here since Cr- and Cr-Mo alloyed steels are frequently sinter hardened, i.e. rapidly cooled after sintering [26, 27], and therefore the critical reaction "window" for N pickup is passed very fast. However, it should also be considered that furnaces with rapid cooling facility usually operate at 1120°C while the high temperature sintering furnaces, which are particularly well suited for sintering of such steels [4, 5], have much lower cooling rates, resulting in more pronounced N pickup. Furthermore, the Cr-Mo steels are also attractive for use in surface densified gears [28] which must not be sinter hardened to retain their deformability, thus being cooled slowly through the critical T range. Especially for these PM parts, which after sintering should be as soft and deformable as possible, nitrogen pickup might prove to be detrimental.

Metallography and microanalysis

Nitrogen is much more soluble in austenite than in ferrite, similar to carbon. The phase transformation during cooling thus should result in precipitation of nitrides. An important task connected to this nitride formation in Astaloy CrM is to identify the location of the nitrides in the specimen. Especially if they appear as precipitates at the grain boundaries, this might affect the properties in a negative way, in a similar way as do proeutectoid cementite or boride precipitates [29]. In the present study, this was mainly investigated for Astaloy CrM- 0.08 %C sintered at 1120°C for 1 h and cooled with 0.5 $K.min^{-1}$. The reason for choosing just this material is the very high amount of nitrogen in this specimen (0.34% nitrogen) combined with almost no carbon after sintering (which would also form visible phases in the microstructure). This makes the identification of the nitrides easier.

First it was checked if nitrides are visible in the microstructures after polishing and etching. The problem occurring here is that it is not possible to distinguish between nitrides and carbides after etching with Nital-Picral (Fig.5). Furthermore in the literature no etching agent is described which only attacks nitrides. This is the reason why a steel with as low carbon content as possible was chosen.

Anyway, there were lots of 'dark dots' seen in the microstructure of Fig.5a the amount of which decreased with higher cooling rate, in parallel to the amount of nitrogen. This can be taken as an indication that these fine particles distributed in the matrix are in fact nitrides.

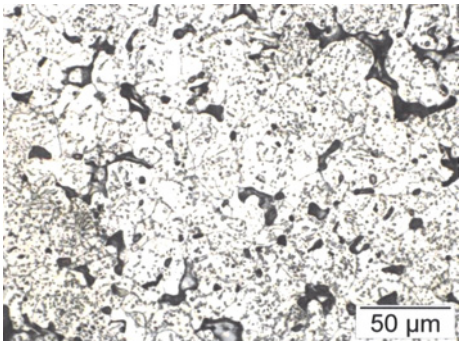

a) cooled with 0.5 $K.min^{-1}$ cooling rate

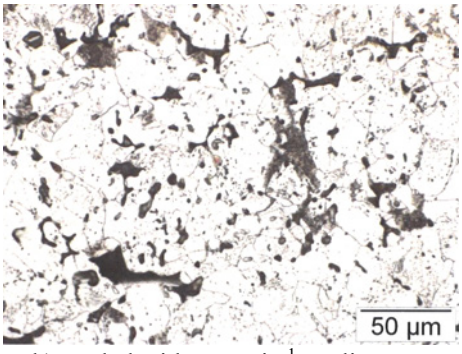

b) cooled with 5 $K.min^{-1}$ cooling rate

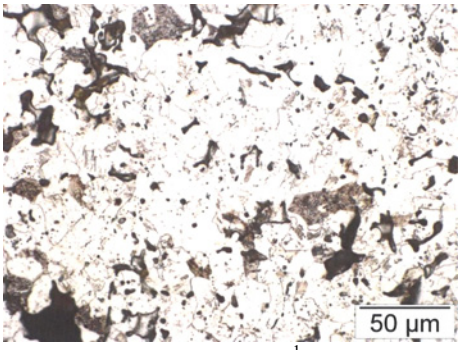

c) cooled with 50 K.min^{-1} cooling rate

Fig.5 a-c. Microstructures of Astaloy CrM-0.08 %C sintered at 1120 °C for 1 h in N_2 and cooled at different rates. Nital-Picral etched.

Furthermore, some investigations were done on fracture surfaces. If there were hard nitride phases at the grain boundaries, intergranular failure should be found on the fracture surface. Moreover it was tried to identify nitrides through EDX analysis, keeping however in mind that nitrogen is one of the light interstitial elements – as also B or C – which are difficult to analyze by energy dispersive detection and therefore end up with with a very high measuring scatter. Furthermore, the EDX analysis was performed on uneven (fracture) surface.

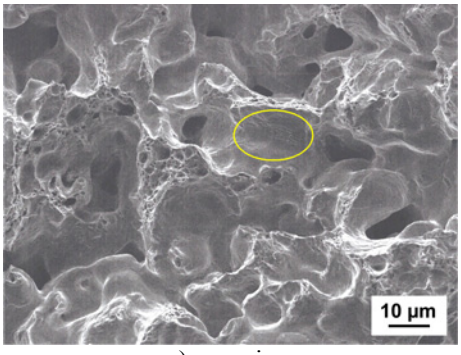

a) overview

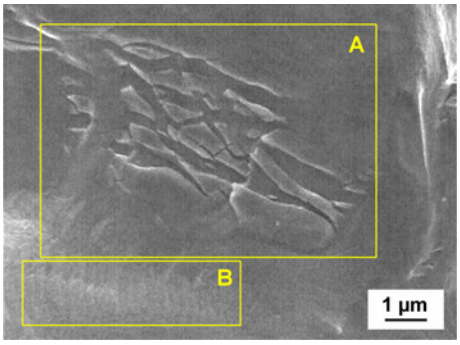

b) magnification of the area marked in Fig.6a

Fig.6 a,b. SEM images of the nitrides at the fracture surface in Astaloy CrM-0.08 %C sintered at 1120°C for 1 h and cooled with 0.5 K.min^{-1}.

Anyway it was possible to draw some conclusions based on the gained results. The nitrides found here are located at pore surfaces, appearing as thin plates (Fig.6). Nitrides at grain and interparticle boundaries should result in intergranular fracture which was not found on the fracture surface.

The nitrides are clearly chromium nitrides and not carbonitrides because of the high presence of Cr and N at the same place in the specimen (Table 4). The carbon content in the nitrogen-rich areas is not higher than in the matrix, which corroborates that in the present case nitrides have been formed and not carbonitrides. This is on one hand in good agreement with the phases expected from the phase diagrams for higher Cr contents [10], in which case thermodynamic calculations by ThermoCalc showed that, as stated above, the

solubility of C and Fe in Cr_2N (hcp) depends on the temperature; in Fig.7a calculation is shown for a high alloy steel in which nitrides are stable at higher temperatures (see also [30, 31]. Since in the present case the nitrides have been precipitated at fairly low temperatures, below 700°C, it would not be surprising that their solubility for C is marginal.

Tab.4. EDX analysis of the nitrides shown in Fig.6b. Astaloy CrM-0.08 %C sintered at 1120°C for 1 h and cooled with 0.5 $K.min^{-1}$.

Area A (second phases)				Area B (matrix as reference)		
Element	Mass%	Atom%		Element	Mass%	Atom%
C K_α	2.08	7.41		C K_α	2.56	10.59
N K_α	7.38	22.39		N K_α	<<	<<
Cr L_α	15.37	12.73		Cr L_α	3.00	2.87
Fe L_α	75.17	57.48		Fe L_α	93,31	83.04

On the other hand, calculations for the composition Fe-3.0%Cr-0.5%Mo-0.3%C-0.35%N (Fig.7c-d) have indicated rather the presence of the cubic phase CrN (fcc) than the hcp phase Cr_2N, which agrees with the ternary system Fe-Cr-N given in [9] and also with experiments on similarly alloyed wrought steels [6, 7]. In this case, the calculations resulted in a nitrogen-carbon ratio in part of almost 1:1 at the lower temperatures, which disagrees with the experimental results. However, the calculation of the compositions (Fig.7b, 7d) shows that the N:C ratio strongly depends on the temperature: At the temperature of the austenite-ferrite transformation the ratio is about 4:1, i.e. very much in favour of nitrogen, and only at lower temperatures the ratio is shifted to almost 1:1. It may therefore be concluded that at the low cooling rates applied here, in the γ-α transformation range N-rich variants of the CrN phase of the type (Cr,Mo)(N,C) are precipitated and that the equilibrium N:C ratio is no more attained during further cooling.

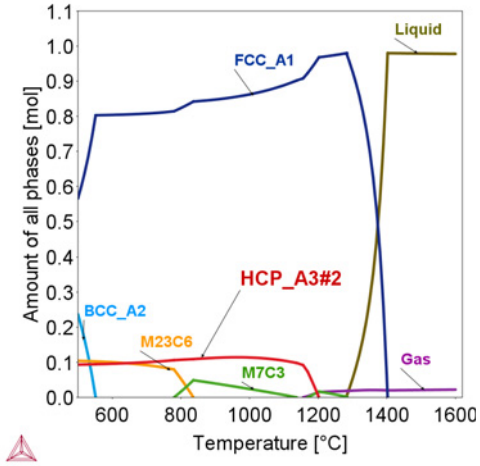

a) Amount of phases in a high alloy steel Fe-20Cr-17Ni-0.5C-0.8N as a function of the temperature

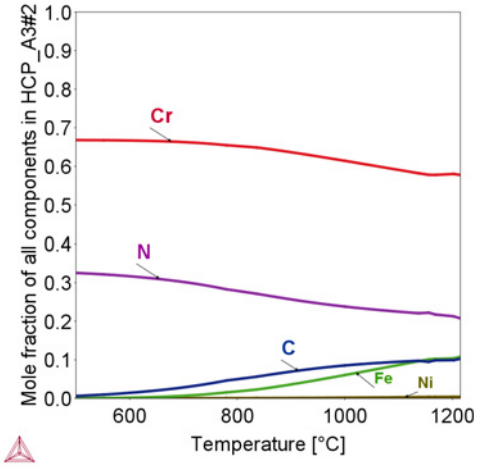

b) Composition of chromium-nitrogen compound in Fe-20Cr-17Ni-0.5C-0.8N as a function of the temperature

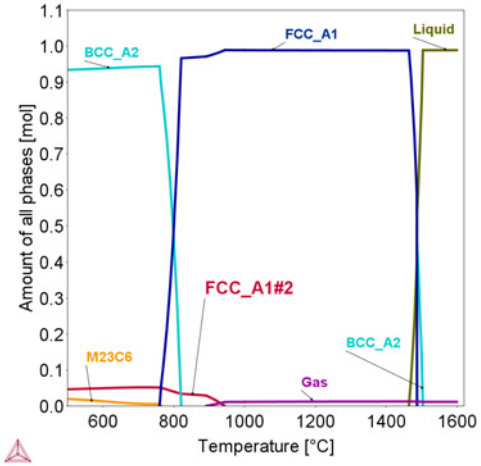

c) Fe-3Cr-0,5Mo-0,30C-0,35N, amount of phases

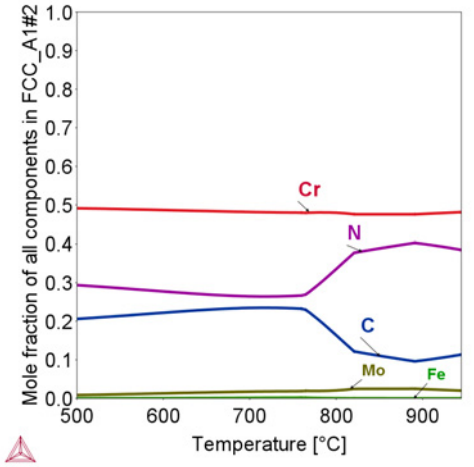

d) as 7c, composition of fcc phases in mol%

Fig.7 a-d. Thermodynamic calculations (ThermoCalc) of the systems Fe-Cr-Ni-C-N and Fe-Cr-Mo-C-N.

A more suitable method to identify the nitrides in a material is a wavelength dispersive detection (WDX). This method provides a significantly better way of detection in the case of light elements such as nitrogen.

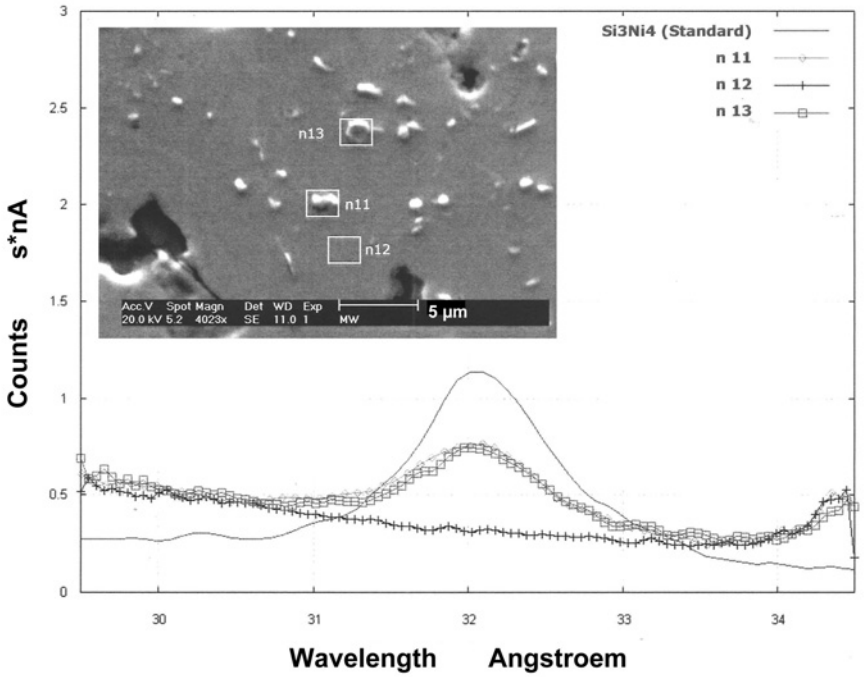

Fig.8. Results of the WDX measurements of Astaloy CrM-0.08%C after sintering at 1120°C and cooling with 0.5 K.min^{-1}

The results of the measurements are shown in comparison to an Si_3N_4 standard, to identify the wavelength at which nitrides are located. It is quite obvious that the particles distributed in the matrix contain nitrogen and therefore are likely to be nitrides. This is also in good agreement with the EDX measurements (Fig.6, Table 4). The matrix itself does not contain any nitrogen (at least not after slow cooling). Due to these findings it can be summarized that the nitrides appear as particles distributed in the matrix or at pore surfaces and not at critical areas like grain boundaries and especially interparticle contacts.

CONCLUSIONS

Sintering of compacts from Astaloy CrM, which is a chromium containing alloy, in nitrogen results in a significant increase of the amount of nitrogen in the material compared to sintering in argon. The reason for this is the tendency of chromium to form nitrides. For such materials the formation of CrN as nitrogen containing phase is expected considering the Fe-Cr-N phase diagram. Even if carbon is present in the material, the formation of separate carbonitrides is not likely, as the concentration of carbon was not higher in areas where nitrogen was mainly concentrated compared to the matrix regions (Figure 4). This is also in good agreement with the phases described in the literature for similar systems [7-10]. On the other hand, the nitride phases may contain significant amounts of carbon depending on the temperature at whch they were formed.

Varying the sintering conditions showed that the nitrogen pickup does not depend on the sintering time, and also the sintering temperature is not too effective. Anyway, sintering at higher temperatures (1250 °C compared to 1120 °C) decreased the amount of nitrogen in the material slightly. The main influencing factor on the amount of nitrogen picked up is the cooling rate. There seems to exist a critical temperature range in which N uptake is favoured. Longer time within this temperature range results in higher amounts of nitrogen in the material. Using thermogravimetry, parallel runs in nitrogen and argon, respectively, indicated that this critical temperature range is correlated to the α to γ / γ to α transformation.

The nitrides formed are located as dispersed particles in the matrix and as thin plates on the pore surfaces. This could be shown using EDAX analyses and WDX analyses. Anyway no nitrides could be found at the grain boundaries, which would be indicated by intergranular failure in the fracture surfaces. This is very beneficial since such grain boundary precipitations could be expected to cause embrittlement.

Summing up it can be said that under commercial sintering and cooling conditions, significant nitrogen pickup and the resulting formation of a large amount of nitrides is not likely, especially when keeping in mind that Astaloy CrM is mainly used as a sinter hardening alloy which experiences high cooling rates. But it has to be considered that keeping the samples for too long times in the critical temperature range can cause a pronounced nitrogen pickup. Anyway, these nitrides are not dangerous for the mechanical properties of the material because they are distributed in the matrix and not contaminating the grain boundaries.

Acknowledgement

This work was carried out in the project “Höganäs Chair in Powder Metallurgy”, round IV, funded and coordinated by Höganäs AB, Sweden. Furthermore, the authors want to thank Dr. Klaudia Hradil, TU Wien X-ray Center, for helpful discussions.

References

[1] Motooka, M., Kuroishi, N., Hara, A., Furukawa, N.: Metal Powder Report, vol. 38,

1983, no. 11, p. 3
[2] Berg, S., Maroli, B. In: Adv. Powder Metall. and Partic. Mater. Proc. PM2002 Orlando. Princeton NJ : MPIF, 2002, on CD
[3] Bergman, O.: Powder Metallurgy, vol. 50, 2007, p. 243
[4] Kremel, S., Danninger, H., Yu, Y.: Powder Metall. Progress, vol. 2, 2002, p. 211
[5] Danninger, H., Gierl, C., Kremel, S., Leitner, G., Jaenicke-Roessler, K., Yu, Y.: Powder Metall. Progress, vol. 3, 2002, p. 125
[6] Van Wiggen, PC., Rozendaal, HCF., Mittemeijer, EJ.: J. Materials Science, vol. 20, 1985, p. 4561
[7] 7. Mittemeijer, EJ.: JOM, vol. 37, 1985, no. 9, p. 16
[8] Fromm, E., Gebhardt, E. In: Gase und Kohlenstoff in Metallen. Berlin Heidelberg New York : Springer-Verlag, 1976, p. 526
[9] Raghavan, VG. In: Phase Diagrams of Iron Ternary Alloys. Vol. 1. Calcutta : The Indian Inst. of Metals, 1984, p. 171
[10] Raghavan, VG.: Phase Diagrams of Quaternary Iron Alloys. Calcutta : The Indian Inst. of Metals, 1996, p. 135
[11] Ettmayer P: Monatsh. Chem. 97 (1966) p.1248
[12] ASM Handbook. Vol.3. Alloy Phase Diagrams. Materials Park OH: ASM, 1992, p.3.26
[13] Šalak, A., et al.: Kovove Mat., vol. 4, 1971, p. 345
[14] Gierl, C., Danninger, H. In: Proc. Euro PM 2005 Prague. Vol. 3. Shrewsbury: EPMA, 2005, p. 1
[15] Bolze, GA., Capus, JM.: Modern Dev. in Powder Metall., vol. 11, 1977, p. 355
[16] Moyer, KH.: Modern Dev. in Powder Metall., vol. 11, 1977, p. 371
[17] Tengzelius, J., Kvist, S-A. In: Proc. PM78 Europ,PM Symp. Stockholm, 1978, p. 46
[18] Bergman, O.: Thesis. Stockholm : KTH, 2008
[19] Bergman, O. In: Proc. EuroPM2001. Vol. 1. Nice, 2001, p .64
[20] Danninger, H., Gierl, C., Leitner, G., Jaenicke-Roessler, K.: P/M Sci. and Technol. Briefs, vol. 6, 2004, no. 3, p. 10
[21] Gmelins Handbuch der Anorganischen Chemie, Eisen. Part A, Abteilung II. System number 59. 8th ed. Berlin : Deutsche Chemische Gesellschaft, Berlin Verlag Chemie, 1934-1939
[22] Benesovsky, F., Hotop, W., Frehn, F.: Planseeber. Pulvermet., vol. 3, 1955, p. 57
[23] Shvab, R., Dudrova, E., Bergman, O., Bengtsson, S.: Powder Metall. Progress, vol. 13, 2013, no. 3-4, p. 103
[24] Shvab, R., Hryha, E., Shykula, P., Bergman, O., Bengtsson, S., Dudrova, E.: Powder Metall. Progress, vol. 14, 2014, no. 2, p. 99
[25] Gmelins Handbuch der Anorganischen Chemie, Eisen, Part A, Abteilung II, System number 59, 8th edition, Deutsche Chemische Gesellschaft, Berlin Verlag Chemie, Berlin (1934-1939)
[26] Yu Y: Proc. EuroPM2001, Nice, EPMA, Shrewsbury (2001) Vol. 1, p.58
[27] Dlapka M, Danninger H, Gierl C, Klammer E, Weiss B, Khatibi G, Betzwar-Kotas A: Int. J. Powder Metall. 48 (2012) No.5, 49-60
[28] Dlapka M, Danninger H, Gierl C, Altena H, Stetina G, Orth P: HTM - Journal of Heat Treatment and Materials 67 (2012) No.2, 158-165
[29] Benesovsky F, Hotop W, Frehn F: Planseeber. Pulvermet. 3 (1955) p.57
[30] Shvab R, Dudrova E, Bergman O, Bengtsson S: Powder Metall. Progress 13 (2013) No.3-4, p.103
[31] Shvab R, Hryha E, Shykula P, Bergman O, Bengtsson S, Dudrova E: Powder Metall. Progress 14 (2014) No.2, p.99